Available online at www.sciencedirect.com

SciVerse ScienceDirect

Ceramics International 39 (2013) 8103–8111

CERAMICS INTERNATIONAL

www.elsevier.com/locate/ceramint

Study of colloidal behaviour and rheology of Al_2O_3–TiO_2 nanosuspensions to obtain free-flowing spray-dried granules for atmospheric plasma spraying

Mónica Vicent[a,*], Enrique Sánchez[a], Gustavo Mallol[a], Rodrigo Moreno[b]

[a]*Instituto de Tecnología Cerámica (ITC), Asociación de Investigación de las Industrias Cerámicas (AICE), Universitat Jaume I (UJI), Castellón, Spain*

[b]*Instituto de Cerámica y Vidrio (ICV), Consejo Superior de Investigaciones Científicas (CSIC), Madrid, Spain*

Received 12 February 2013; received in revised form 22 March 2013; accepted 25 March 2013
Available online 6 April 2013

Abstract

This work deals with the dispersion and stabilisation of nanosized Al_2O_3 and TiO_2 particles in aqueous medium. The dispersing conditions were studied as a function of pH, dispersant content, solid loading and ageing.

Well-dispersed nanosuspensions of Al_2O_3 with solids contents up to 15 vol.% and TiO_2 with solids contents up to 30 vol.% were obtained by dispersing each type of nanoparticles with 4 wt% of polyacrylic acid-based polyelectrolyte. In order to obtain a concentrated 87 wt% Al_2O_3–13 wt% TiO_2 suspension, a 15 vol.% homogeneous nanosuspension, composed by alumina and titania nanopowders, was prepared and then reconstituted by spray-drying into free-flowing powders. This spray-dried powder showed an adequate granule size distribution, a very high flowability and a reasonable density for diverse purposes, such as to be used in atmospheric plasma spraying as a feedstock to obtain nanostructured coatings.

Keywords: A. Suspensions; Spray-drying; Nanoparticle; Al_2O_3–TiO_2

1. Introduction

In the last few years, nanopowders (i.e. powders comprising particles smaller than 100 nm) have revolutionised a great number of devices and processes, because at this scale unique optical, magnetic, electrical, and other properties emerge. The unique properties of nanoparticles thus make them of great interest for new product development. Much research is consequently being conducted to develop nanostructured materials that exhibit enhanced properties compared to those of their submicron- or micron-sized counterparts.

Nanoparticles sometimes need to be dispersed in a liquid medium for different purposes and applications. However, the potential benefits of such nanoparticles can only be realised if the particles are well dispersed in the medium.

When nanostructured coatings are to be obtained by atmospheric plasma spraying (APS), a widely used thermal spray method for producing coatings, nanoparticles need to be used as raw material. However, nanoparticles cannot be directly plasma sprayed, owing to their small mass and poor flowability. As a result, the nanoparticles need to be agglomerated to form sprayable micrometre-sized granules. This stage is critical for the success of the coating process and for the final properties of the coatings [1].

Alumina (Al_2O_3) is a hard material commonly used for tribological applications. Deposition of Al_2O_3 onto surfaces of mechanical parts by the plasma spray technique effectively enables the surface functionality of engineering parts to be improved. Al_2O_3-based nanocomposite coatings have been extensively studied, particularly those containing TiO_2 [1,2]. Al_2O_3–TiO_2 coatings are of interest because they exhibit better toughness and wear resistance than monolithic Al_2O_3 coatings [2]. A widely used typical mixture in APS is 87 wt% Al_2O_3–13 wt% TiO_2 [1]. Nanostructured coatings based on this mixture yield enhanced coating properties, such as wear performance, compared to conventional (microstructured) coatings [3].

Although many authors have examined how slurry formulation affects the characteristics of the resulting ceramic granules, few studies are reported on spray-dried powders for

*Corresponding author. Tel.: +34 964 34 24 24; fax: +34 964 34 24 25.
E-mail addresses: mvicent@itc.uji.es, monica.vicent@itc.uji.es (M. Vicent).

0272-8842/$ - see front matter
http://dx.doi.org/10.1016/j.ceramint.2013.03.083

thermal spraying [4,5]. Most studies using nanostructured spray-dried feedstock only mention the agglomeration process, without providing any details on the nanoparticle suspension preparation and spray-drying operation. The correlation between agglomeration process variables, agglomerate characteristics, and coating microstructure and properties is therefore far from being well established. This first requires investigation of the colloidal behaviour and rheology of the ceramic oxide system involved. These aspects have been extensively studied for titania nanosuspensions in recent years [6,7], also by some authors of this paper [8–10]. However, nanosuspensions of Al_2O_3 have drawn less attention, probably because of the difficulty of making relatively concentrated suspensions of this oxide [11–13]. However, studies on the nanosuspension preparation of Al_2O_3–TiO_2 mixtures are unavailable in the literature.

This study was therefore undertaken to prepare Al_2O_3–TiO_2 spray-dried granules from aqueous suspensions of nanosized powders. These spray-dried granules are intended for use in manufacturing nanostructured APS coatings, as reported elsewhere [1–3]. The colloidal behaviour of titania nanopowders in water was reported in a previous study [8]. In that study, a commercial salt of polyacrylic acid-based polyelectrolyte was successfully used for the preparation of concentrated suspensions [8,9]. In the present study, the colloidal stability of alumina nanopowders in water, using the same polyelectrolyte as in the case of TiO_2, was investigated. Once the alumina suspensions had been studied and optimised, a well-dispersed, concentrated nanosuspension of 87 wt% Al_2O_3–13 wt% TiO_2 mixture was prepared and subsequently spray-dried. The resulting spray-dried powder was fully characterised to assess its feasibility for use as feedstock to obtain nanostructured coatings by APS.

2. Experimental

2.1. Starting raw material characterisation

Commercial nanopowders of alumina and titania (Aeroxide® AluC and Aeroxide® P25, both supplied by Degussa-Evonik, Germany) were employed in this study. The main physicochemical characteristics, as provided by the supplier, are shown in Table 1.

AluC-nanopowder is produced via high-temperature flame hydrolysis following an analogous route to the AEROSIL® -process developed by its supplier (this process succeeded in producing the first ultrafine-particle pyrogenic powder). AluC is a very fine fumed metal oxide with a high specific surface area and is made up of a mixture of δ/γ-alumina phase. P25-nanopowder is a titanium dioxide which is also manufactured according to the AEROSIL®-process. It is a reference TiO_2 standard material that has been widely used in many photocatalytic studies and contains anatase and rutile phases in a ratio of about 3:1 [14].

Table 1
Commercial nanoparticle characteristics (information provided by the supplier).

Property	AEROXIDE® AluC	AEROXIDE® P25
Average particle size, d_{50} (nm)	13	21
Specific surface area (m^2/g)	100 ± 15	50 ± 15
pH in 4% dispersion	4.5–5.5	3.5–4.5
Purity (wt%)	99.6	99.5

Both nanopowders were characterised by transmission electronic microscopy, TEM (H7100, Hitachi, Japan and CM10, Philips, Netherlands) and the specific surface area was determined using the single-point BET method (Monosorb, Quantachrome Co., USA).

2.2. Colloidal behaviour characterisation

The colloidal stability of Al_2O_3 was studied measuring the zeta potential as a function of deflocculant content and pH using a dynamic light scattering instrument (Zetasizer NanoZS, Malvern, UK), based on the laser Doppler velocimetry technique. The deflocculant used was a commercial salt (DURAMAX™ D-3005, Rohm & Haas, USA) of polyacrylic acid-based polyelectrolyte (PAA), with 35 wt% of active matter.

Different Al_2O_3 dilutions were tested to measure zeta potential with the best accuracy, which was reached for a concentration of 0.01 wt% alumina, using KCl 0.01 M as inert electrolyte. pH values were determined with a pH-meter (716 DMS Titrine, Metrohm, Switzerland) and were adjusted with HCl and KOH solutions (0.1 and 0.01 M). To improve the dispersion state, different sonication times were tested using an ultrasounds probe (UP 400 S, Dr Hielscher GmbH, Germany) in order to avoid agglomerates formation. A sonication time of 30 s was found to be optimum for the preparation of diluted suspensions for zeta potential measurements. Note that the ultrasounds, in this case, were applied to 60-mL aliquots of every nanosuspension and using an ice bath to avoid excessive heating.

2.3. Rheological study

First of all, nanoparticles suspensions were prepared by adding the nanoparticles in the dispersing medium (deionised water containing the optimum quantity of dispersant) using a blade-stirrer. Preliminary test showed that these stirring conditions are insufficient to completely deagglomerate the powder for low solids content suspensions. Thus, the suspensions were dispersed with an ultrasound probe in order to break down any present agglomerates. Different periods of ultrasounds (US) exposure were investigated, from 0 to 5 min in 20-mL aliquots of each nanosuspension.

The rheological behaviour of all nanosuspensions was determined using a rheometer (Haake RS50, Thermo, Karlsruhe, Germany) operating at controlled shear rate (CR) by loading the shear rate from 0 to 1000 s^{-1} in 5 min, maintaining at 1000 s^{-1} for 1 min and downloading from 1000 to 0 s^{-1} in 5 min. The measurements were performed at 25 °C using a double-cone and plate system. The thixotropy values were

taken from CR curves, measuring the area enclosed between ascending and descending ramps in the described flow curves.

Finally, the effect of ageing on the nanosuspension's characteristics was studied by maintaining them at low speed agitation in a closed flask into a horizontal shaker, for later measurements. The rheological behaviour of the nanosuspensions was checked for ageing times up to 7 days.

2.4. Spray-drying process

As mentioned before, it is necessary to agglomerate the nanoparticles into sprayable micrometric-sized granules, previously to their deposition by APS to form nanostructured coatings. Actually, nanoparticles cannot be directly fed into the plasma torch. Thus spray-dried granules were obtained from 87 wt% Al_2O_3–13 wt% TiO_2 (15 vol.%) suspension in a spray-dryer (Mobile Minor, Gea Niro, Denmark) with a drying capacity of 7 kg water/h [1,8,9]. At this solids content, suspension viscosity was suitable for spray-drying in the pilot equipment.

2.5. Spray-dried powder characterisation

Spray-dried granules were fully characterised. The granule size distribution was measured by laser light scattering (Mastersizer S, Malvern, UK). A small quantity of powder was dispersed in an aqueous medium using a deflocculant (Dolapix CE-64, Zschimmer-Schwarz, Germany) and the preparation of the samples was made by three methods: shaking for 5 min without sonication, and for 1 and 5 min with sonication. It should be pointed out that, contrarily to the preparation of suspensions for zeta potential and rheological measurements, the measurement of granule size distribution was performed using an ultrasounds bath (instead of an sonication probe) to avoid the breakdown of the granules into their primary particles.

Agglomerate apparent density was calculated from tapped powder density by assuming a theoretical packing factor of 0.6, which is a characteristic of monosize, spherical particles [15]. Specific surface area and pore structure were determined using a nitrogen gas adsorption technique (TriStar 3000, Micromeritics, USA) although pore structure was also evaluated by mercury intrusion porosimetry, MIP (AutoPore IV 9500, Micromeritics, USA). A field emission environmental scanning electron microscope, FEG-ESEM (QUANTA 200FEG, FEI Company, USA) equipped with an energy-dispersive X-ray spectrometer (EDAX Genesis) was used to examine the feedstock microstructure.

In addition, powder flowability was estimated. Several methods are used to evaluate the flow properties of powder materials: the most accurate are based on the assessment of the rheological behaviour of the powders subjected to normal and shear stress [16]. For a powder to flow, the applied shear stress needs to be larger than a threshold value or yield stress (just as in plastic fluids). However, unlike the latter, the magnitude of the threshold shear stress depends on the consolidation conditions to which the powder bed has been subjected and on the normal stress that acts upon the shear plane when bed

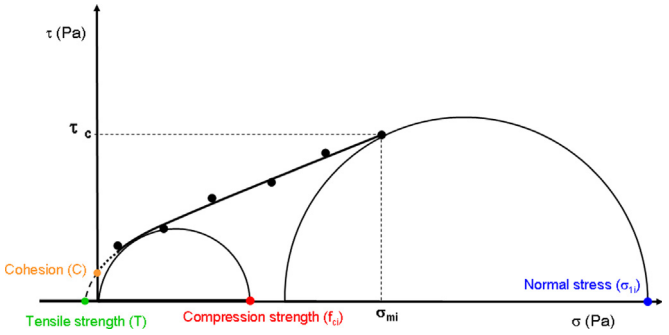

Fig. 1. Hypothetical experiment to illustrate the different types of mechanical strength of the bed and calculation of σ_1, C, T and f_C.

Table 2
Flow behaviour with respect to the flow factor (ffc) according to Jenike.

ffc	< 1	1–2	2–4	4–10	> 10
Behaviour	No flow	Very cohesive	Cohesive	Easy flowing	Free flowing

flow or rupture commences. Therefore, in this method, the flowability characterisation is based on determining, for a given bed compactness (ϕ), the variation of shear stress (τ) with normal stress (σ) known as the flow curve or yield loci (Fig. 1), according to Jenike and Johanson [17]. The flow curve allows the calculation of three types of mechanical strength of the bed when normal stress (σ_1) is applied: shear or cohesive strength (C), tensile strength (T) and compressive strength (f_C).

When measuring flow curves at different compactness values, pairs of values (f_C, σ_1) are obtained; the representation of those pairs of values is the material flow function (MFF). Normally the MFF fits properly to a straight line according to Eq. (1).

$$f_C = f_{C0} + \alpha\sigma_1 \quad (1)$$

where f_{C0} and α are directly related to the material's flowability. Higher f_{C0} and slope indicate a lower powder's flowability.

Jenike proposed the quotient σ_1/f_C which is called flow factor (ffc), and is probably the most widely used index to define the flowability of particulate materials, since it allows them to be classified as a function of their flowability (Table 2).

This flowability test was carried out in a rotational split level shear tester (RO-200 Automatic, IPT Industrial Powder Technology, Liechtenstein). For comparison purpose an estimate of the powder flowability based on the determination of the Hausner index was also carried out. The determination of this index has been set out elsewhere [15].

Since the targeted application for this spray-dried powder deals with APS coatings, powder requirements concerning agglomerate size distribution and density as well as powder flowability must be achieved. According to literature relatively dense (higher than 1000 kg/m^3 apparent density), free-flowing

agglomerates with an agglomerate size distribution ranging from 15 to 200 μm are necessary for a suitable feeding into the plasma torch [4,18,19]. It is worthwhile noticing that the target values of these parameters exclusively rely on the common practice.

3. Results and discussion

3.1. Starting raw material characterisation and its colloidal behaviour

Both nanopowders were observed by TEM. Regarding AluC, nanoparticles of 10–15 nm size were observed (Fig. 2). The microstructure observation of the P25 nanopowder was already reported in a previous work, which showed that the particles were agglomerated and displayed a primary particles size of approximately 20–40 nm [8]. Thus, both AluC and P25 can be considered as nanopowders constituted by agglomerated nanoparticles.

The specific surface areas of AluC and P25, measured by BET, are 102 and 48.5 m^2/g, respectively. These values as well as TEM observations agree with the data provided by the supplier (Table 1).

In order to deagglomerate and stabilise the nanoparticles in water, an ammonium polyacrylate (PAA) was used, as it has been shown to be effective for suspensions of P25-titania nanoparticles [8]. Fig. 3 shows the evolution of zeta potential of the alumina nanopowders as a function of pH for suspensions without and with 1, 2 and 4 wt% PAA. The IEP of the AluC nanopowder occurs at pH around 9, in good agreement with the values typically reported in the literature [20]. The IEP shifts to acidic pHs as the concentration of PAA increases until a value of the IEP of ~4 is reached when 4 wt% PAA is added. The evolution of zeta potential with pH depends on the dispersant concentration which shifts the IEP. These results indicate that it adsorbs on the particles surface and it is a suitable deflocculant for this raw material. PAA specifically adsorbs and leads to well dispersed alumina nanosuspensions above pH=6, if a 4 wt% proportion is used.

Table 3 shows the isoelectric point (IEP) values obtained with different PAA concentrations (1, 2 and 4 wt% PAA) for AluC and P25 nanosuspensions. A similar decrease in the IEP towards acidic values was observed in both suspensions and demonstrates that the largest values of zeta potential and, thus, maximum stability occur at neutral and alkaline pH values (at broad pH interval). For this reason, PAA is a good dispersant for both alumina and titania nanopowders [8,9] and the optimum concentration is, in both cases, 4 wt% PAA.

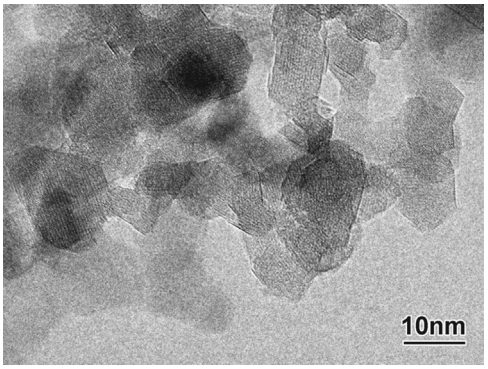

Fig. 2. TEM micrograph of Al_2O_3 nanoparticles (AEROXIDE® AluC).

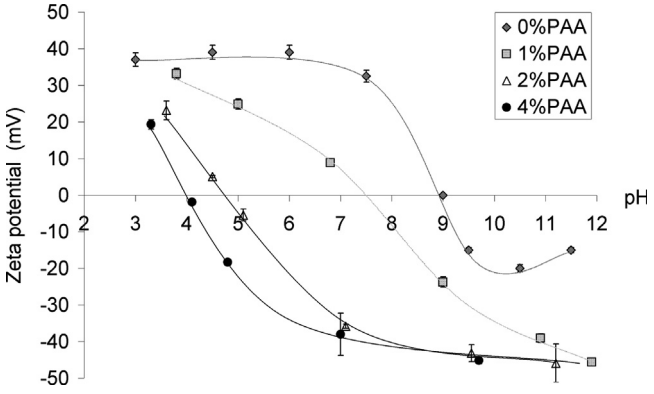

Fig. 3. Effect of PAA addition on the evolution of zeta potential with pH (AluC).

Table 3
IEP value obtained for every PAA proportion.

	PAA (wt%)			
	0	1	2	4
AluC	9	7.2	5	4
P25	7.2	4	3.8	2.7

3.2. Rheological study

The rheological behaviour of titania suspension (dispersing P25 nanoparticles in water) was already evaluated in a previous work [8] whereas, in the present work, the effect of sonication time and ageing time on the rheological behaviour of concentrated nanoalumina suspensions was determined. Finally, a study of the mixture is also detailed in this section.

Effect of ultrasounds in AluC-suspensions. Sonication application plays a key role on the dispersion of nanoparticles [8,9]. In fact, too short sonication times might not be enough to prepare homogeneous suspensions, whereas excessively long times might produce agglomeration. Because of that, the sonication time needs to be optimised for each system.

Fig. 4 shows the rheological behaviour of 15 vol.% (~39.2 wt %) solids content alumina suspensions. A broad thixotropic cycle is observed when no sonication is used. Moreover, in this case, it was not possible to measure all the points of upward flow curve due to the excessively high viscosity of no-sonication nanosuspension, which leads to values out of the range of the torque of the instrument. As expected, it can be observed that sonicated suspensions show lower viscosity and less thixotropy. However, the thixotropy is still relatively high due to the surface area of these nanopowders, which makes the preparation of concentrated suspensions difficult. According to shear stress–shear rate curves

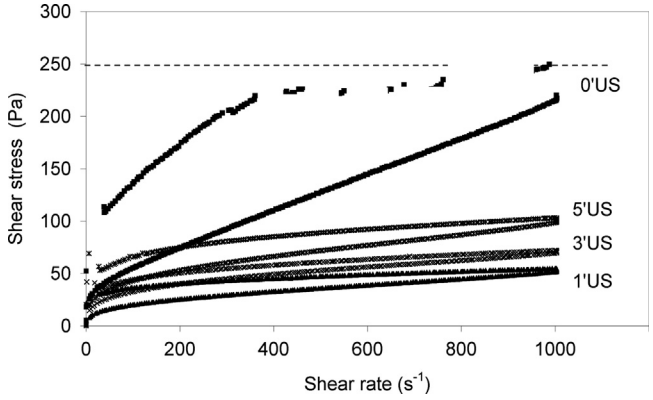

Fig. 4. Effect of sonication time on the flow curves of 15 vol.% Al_2O_3 suspensions.

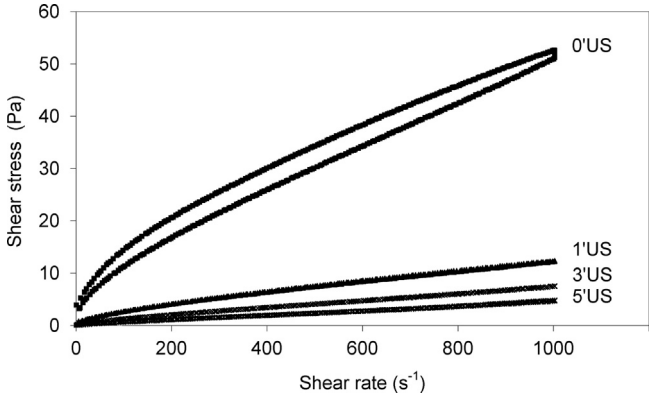

Fig. 5. Effect of sonication time on the flow curves of 15 vol.% TiO_2 suspensions.

Table 4
Thixotropy values of alumina and titania suspensions.

Sonication time (min)	Thixotropy (Pa/s)	
	AluC-nanosuspension (15 vol.%)	P25-nanosuspension (15 vol.%)
0	114,600	3,580
1	11,180	150
3	8,530	36
5	16,570	74

(Fig. 4) and thixotropy values (Table 4), the optimum sonication time for 15 vol.% alumina nanosuspension was 1 min. The further increase of viscosity with sonication time could be related to a re-agglomeration effect of the more active surfaces as a consequence of the reduction of interparticle distances. As a consequence they cannot overcome the strong overheating induced by the sonication probe.

Fig. 5 shows the rheological behaviour of 15 vol.% (~39.9 wt %) solids content P25-suspensions as-prepared and after dispersion with ultrasounds for 1, 3 and 5 min. The 15 vol.% suspensions prepared herein exhibited very low viscosities after sonication, and displayed decreasing viscosity with sonication time up to 5 min. In this case, the thixotropy values (Table 4) are within the measurement error, so that it can be assumed that sonicated suspensions have no thixotropy. Additionally, as it was demonstrated in previous works, well-dispersed, concentrated P25-nanopowder suspensions can be prepared up to 30 vol.% solids loading in water [8] and up to 35 vol.% solid loading with a commercial titania nanosuspension [9].

According to above results, in both suspensions, the viscosity decreases when sonication time increases until an optimum time from which viscosity increases again. The best dispersion is achieved with 1 min ultrasounds for 15 vol.% alumina suspensions, and any sonication time between 1 and 5 min for titania suspensions.

Effect of ageing in AluC-suspensions. This study was carried out in all the samples (at different sonication times and solids contents). The findings are set out in Figs. 6 and 7.

In the case of the ageing behaviour of 10 vol.% nanosuspensions, due to its moderate viscosity, only the effect of fresh and 7 days-aged suspensions on the flow curves for different sonications is shown (Fig. 6). As it can be seen there is a slight increase of thixotropy with time but the suspension hardly deteriorates. In fact, the sonicated suspensions displayed a fairly stable viscosity after ageing. This is an important issue, since many suspensions prepared from nanosized powders become gel in hours or even in minutes.

In the case of the ageing behaviour of 15 vol.% nanosuspensions (Fig. 7), the behaviour is different. As it can be observed after 1 week the viscosity of non-sonicated suspension strongly increases. However, in the case of sonicated suspensions, the viscosity and the thixotropy increase are much less sharp than those of the non-sonicated suspension. A possible explanation stand on the fact that the starting viscosity is much higher than that of 10 vol.% and thus, the tendency to sedimentation and/or agglomeration is much lower due to the lower mobility of the particles inside the suspension structure.

Al_2O_3–TiO_2 mixture. Fig. 8 shows the rheological behaviour of 87 wt% Al_2O_3–13 wt% TiO_2 nanosuspension for 15 vol.% as-prepared and after exposure to ultrasounds probe for 1, 3 and 5 min. The viscosity of the as-prepared 15 vol.% mixture suspension strongly decreases with sonication time for 1 min and for 3 min; finally further sonication up to 5 min produces a very small reduction. The same behaviour is observed in the thixotropy values (Table 5, first column).

Thus, viscosities values of 15 vol.% mixture suspension are lower than those of 15 vol.% AluC-nanosuspension because the addition of a low-viscosity TiO_2 suspension (15 vol.% P25-nanosuspension) considerably contributes to decrease the viscosity of the mixture. For this reason, the mixture could be measured without using sonication time whereas 15 vol.% Al_2O_3 nanosuspension could not be prepared in these conditions because of its high viscosity (Fig. 4).

With regard to ageing of Al_2O_3–TiO_2 mixture nanosuspension, thixotropy values are shown in Table 5. For every sonication time applied, the thixotropy of nanosuspension increases when the sample is left at rest, the highest value being obtained after 7 days. As the sample ages with time it should be used immediately after preparation.

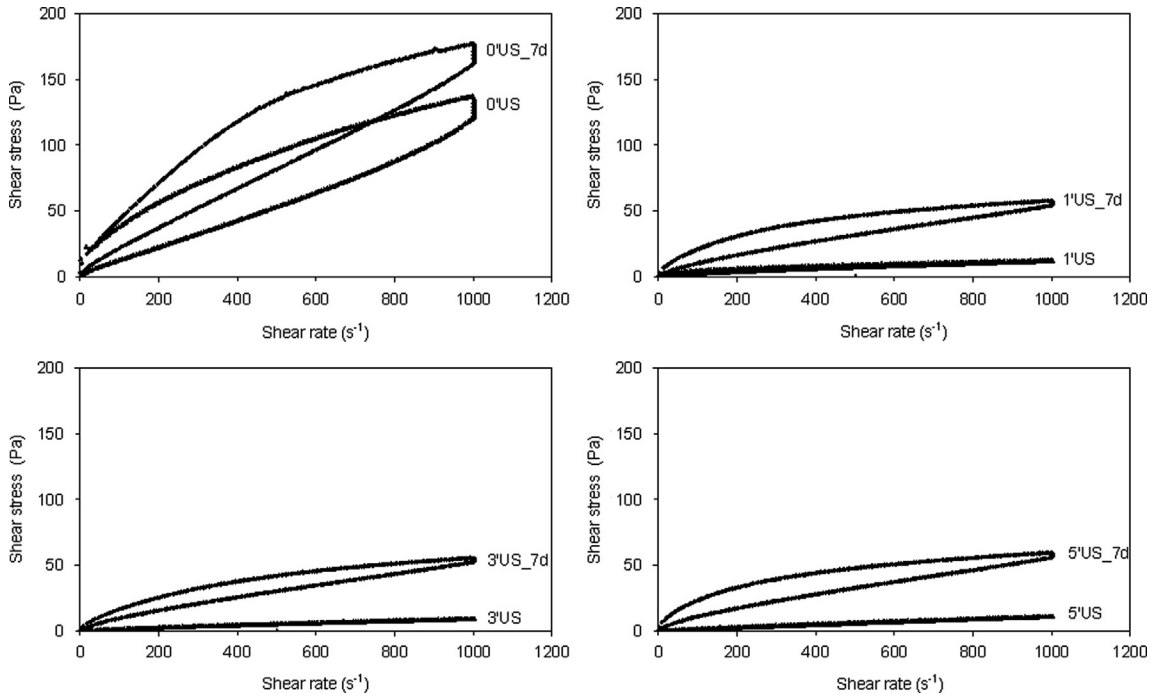

Fig. 6. Effect of ageing (7 days) for every sonication time (0, 1, 3 and 5 min) on the flow curves of 10 vol.% AluC-nanosuspensions.

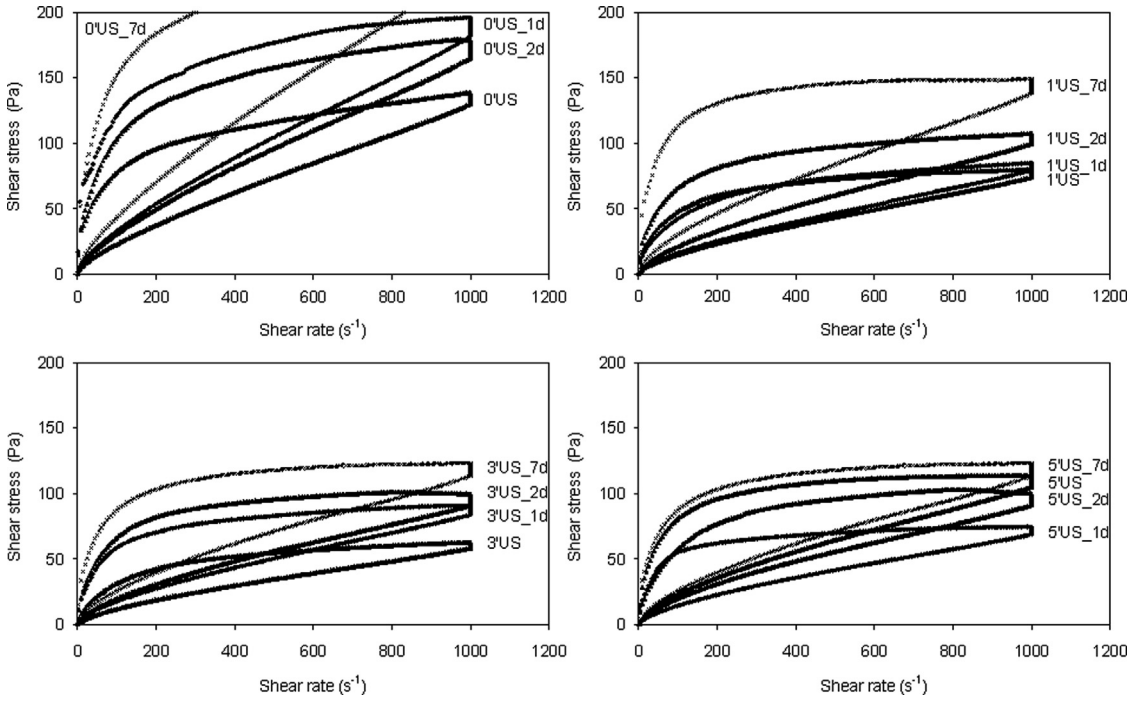

Fig. 7. Effect of ageing (1, 2 and 7 days) for every sonication time (0, 1, 3 and 5 min) on the flow curves of 15 vol.% AluC-nanosuspensions.

3.3. Spray-dried powder characterisation

A nanosuspension of the 87 wt% Al_2O_3–13 wt% TiO_2 mixture for spray-drying was obtained. The optimised 15 vol.% Al_2O_3–TiO_2 nanosuspension was spray-dried, being its viscosity suitable for spray-drying in the pilot equipment set out above. As the suspension was spray-dried immediately after its preparation no sonication was necessary.

FEG-ESEM micrographs at different magnifications (Fig. 9) reveal that granules are highly spherical meanwhile the typical doughnut-shape of spray-dried granules are clearly observed. At high magnifications, it can be confirmed that the granules are built up of glued nanoparticles in a relatively quite loose packing [1,8,9].

Powder granule size distribution (Fig. 10), measured by laser diffraction, confirms the micrometre size range of the

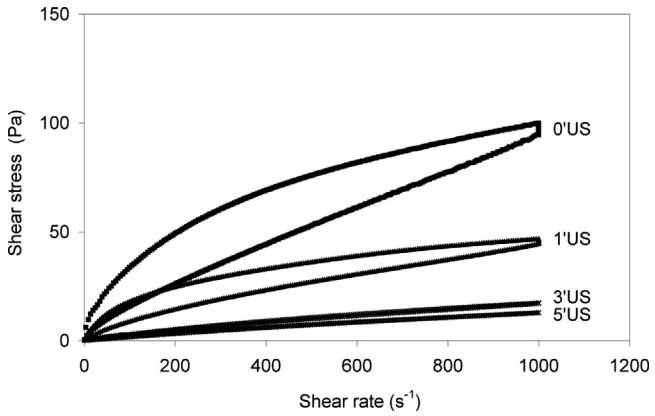

Fig. 8. Flow curves of dispersed 87 wt% Al_2O_3–13 wt% TiO_2 nanosuspension (15 vol.%).

Table 5
Thixotropy values of 87 wt% AluC–13 wt% P25 (15 vol.%) nanosuspensions, just as prepared and after different aging times (1, 2 and 7 days).

Sonication time (min)	Thixotropy (Pa/s)			
	As prepared ($t=0$)	1 day	2 days	7 days
0	18,270	38,990	49,710	65,300
1	7,820	25,970	31,780	39,280
3	506	14,920	15,260	28,810
5	–	10,960	13,860	22,250

spray-dried agglomerates. As set out in Section 2.5, three methods of sample dispersion in water were followed in order to assess the integrity of the agglomerates: 1 or 5 min of ultrasounds bath and 5 min of simple manual shaking. As expected ultrasounds (US) break down the granules, although 1 min ultrasounds show very little breaking effect when compared with hand shaking. According to the manual shaking curve, agglomerates display a monomodal granule size distribution with a mean size around 100–140 μm. This size distribution agrees with the standard requirements of APS feedstocks as set out above.

Table 6 details some characteristics of the spray-dried granules, including: agglomerate apparent density estimated from filling/tapping powder density, specific surface area (measured by nitrogen adsorption at 77 K, BET method), mean pore diameter obtained by nitrogen gas adsorption (BJH method) and powder mean pore diameters corresponding to intergranular and intragranular porosities measured by mercury porosimetry.

The pore size distribution measured by nitrogen gas adsorption, Barret–Joyner–Halenda (BJH) method, only determines the intragranular porosity. On contrary, mercury porosimetry evaluates both inter- and intra-porosity of the granules. Nevertheless, the agreement between the values obtained from the two methods (16.2 nm and 20 nm for BJH and mercury pore sizing methods respectively) is very good, confirming at the same time the nanostructured character of the obtained agglomerates. On the other hand, intergranular porosity is associated with large pores between granules. This type of porosity, which largely depends on the sample preparation for porosimetry test, shows scarce interest for APS process since the powder is fed into the plasma torch without any compacting effect.

Finally, agglomerate apparent density was 1150 kg/m^3 which also fulfils the density requirements of an agglomerated feedstock for APS process as previously set out.

Furthermore, high powder flowability is also required to guarantee a homogeneous feeding of the feedstock into plasma torch, by allowing a continuous and constant powder mass flow. To evaluate the flowability, flow curves were obtained at three different compressive stresses. The results are tabulated in Table 7.

From the flow curves the compressive strength (f_C) and the normal stress (σ_1) are calculated to represent the MFF (material flow function) as set out in Section 2.5. Fig. 11 compares the MFF of the tested spray-dried powder and of other two model materials which are widely used in industry [21,22]: an easy-flowing powder (spray-dried powder for tile manufacture) and a very cohesive powder (zinc oxide).

Table 8 shows rheological parameters and flow behaviour, according to Jenike, for each material. The compression strength and the flow factor were calculated at 10 kPa of normal stress.

Zinc oxide powder is a pulverulent ceramic material with high compression strength and its behaviour is classified as very cohesive. The spray-dried powder for tile manufacturing shows an easy-flowing behaviour (required for filling the dies in pressing stage). The spray-dried powder obtained in this research displays even a better behaviour than that of a traditional ceramic spray-dried powder, being classified as free flowing powder. Thus, this feedstock exhibits an excellent flowability so as to be transported to and fed into a plasma torch in APS processes.

In order to compare these findings with flowability results obtained in previous research, and based on the evaluation of the Hausner index [1,8,9], the value of this index was experimentally determined. As expected, the Hausner ratio obtained was 1.10 ± 0.03 which confirms the good flowablity of the obtained powder since free-flowing powder is considered when Hausner ratio is < 1.25 [23].

4. Conclusions

In this work, dispersion and stabilisation of alumina nanoparticles (AluC) in water were studied using a commercial salt of polyacrylic acid-based polyelectrolyte (PAA). Moreover, it was previously established that, this dispersant can also be used to stabilise titania nanoparticles (P25) in water. As a consequence, an Al_2O_3–TiO_2 nanosuspension with a weight ratio of 87–13 was successfully prepared using the same dispersant.

Rheological behaviour of a 15 vol.% mixture dispersed by sonication indicates a high stability. Moreover the suspension presented a suitable viscosity for the subsequent spray-drying process. After spray-drying, typical doughnut-shape, micrometre-sized agglomerates were obtained in which the nanoparticles were packed in a relatively loose assembly. The

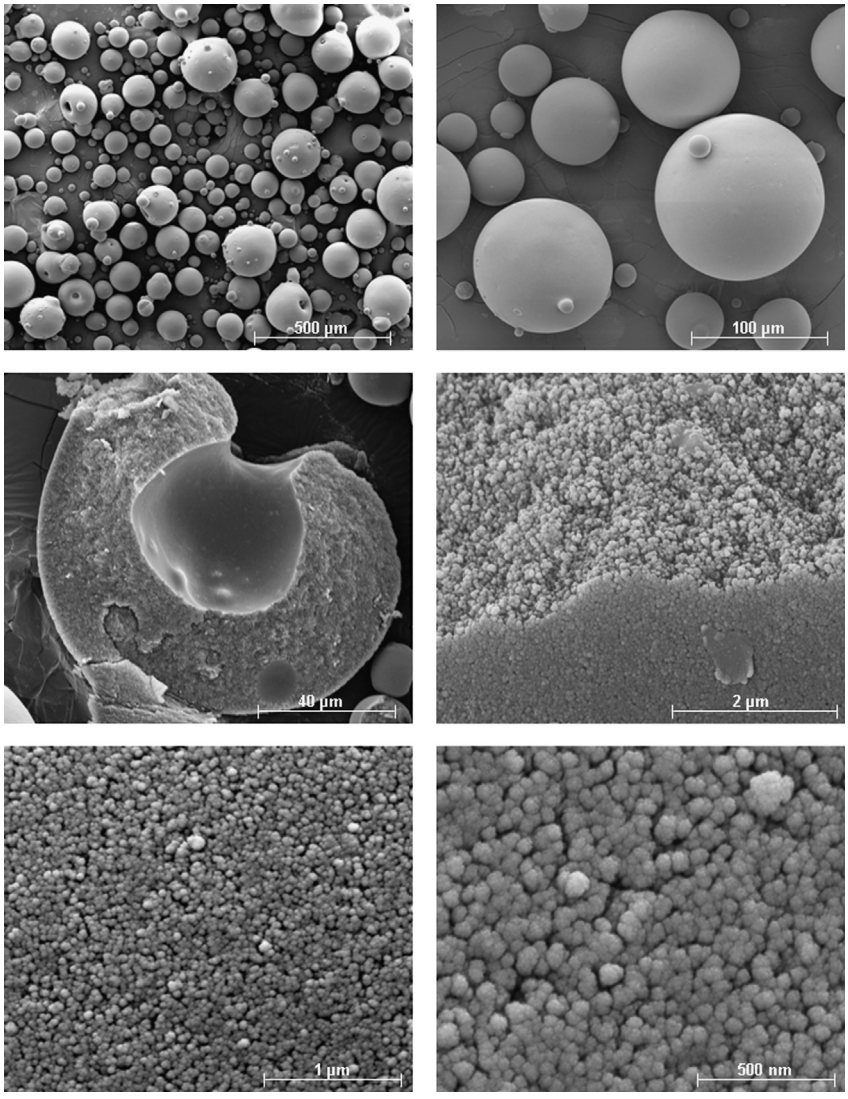

Fig. 9. FEG-ESEM micrographs of the obtained spray-dried powder at different magnifications.

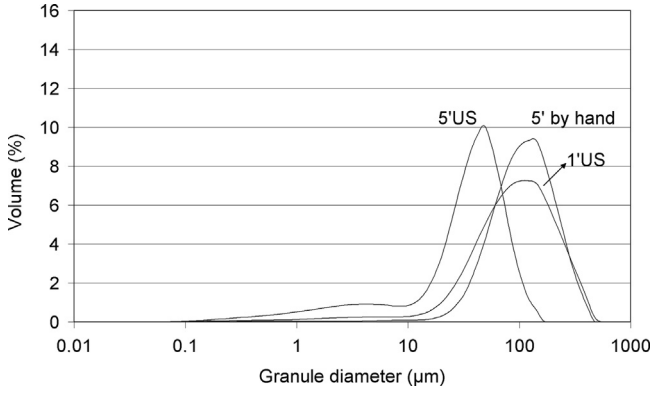

Fig. 10. Granule size distribution of the spray-dried powder obtained by different methods of sample preparation.

Table 6
Some characteristics of the spray-dried granules obtained from 15 vol.% nanosuspensions.

			Spray-dried powder
Powder filling/tapping density	Granule apparent density	ρ_G (g/cm^3)	1.15
N_2 adsorption/desorption isotherm	BET method	S_s (m^2/g)	94
	BJH method	D_{pore} (nm)	16.2
Porosimetry	Mean pore size (µm)	$D_{Intergranular}$	20.4
		$D_{Intragranular}$	0.02

nanostructured character of the spray-dried agglomerates was also confirmed by pore-sizing techniques.

The agglomerates characteristics include a relatively narrow size distribution with a mean agglomerate size around 120 µm, an acceptable density and an excellent flowability, which make them very adequate to be used as feedstock to obtain nanostructured coatings by atmospheric plasma spraying. For this last application, Al_2O_3–TiO_2 system is widely used, mainly to obtain tribological coatings.

Table 7
Flow curve values for the spray-dried powder obtained at three different compressive stresses by means of the shear tester.

σ_C=3 kPa		σ_C=6 kPa		σ_C=9 kPa	
σ (kPa))	τ (kPa)	σ (kPa)	τ (kPa)	σ (kPa)	τ (kPa)
3.0	1.5	6.0	3.1	9.0	4.6
2.5	1.2	5.0	2.6	7.0	3.6
2.0	1.1	4.0	2.0	5.0	2.6
1.5	0.8	3.0	1.5	3.0	1.6
1.0	0.6	2.0	1.0	1.0	0.6
–	–	1.0	0.6	–	–

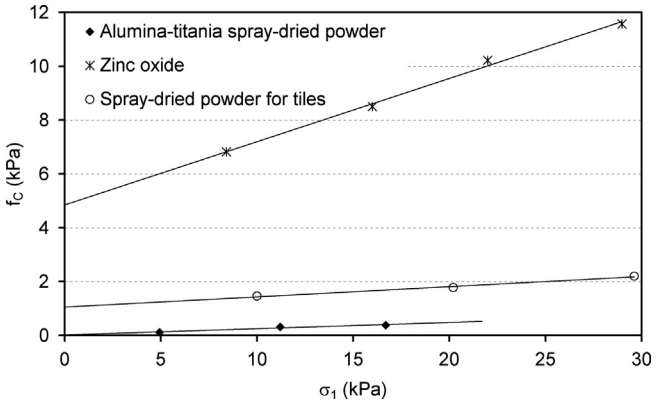

Fig. 11. MFFs of the spray-dried powder together with two industrial model powders.

Table 8
Rheological parameters and flow behaviour according to Jenike for each material (spray-dried powder and the two model powders).

Material	α	f_{C0} (kPa)	$f_C^{10\ kPa}$ (kPa)	$ff_C^{10\ kPa}$	Behaviour
Zinc oxide [21,22]	0.235	4.85	7.20	1.4	Very cohesive
Spray-dried powder for tiles [21,22]	0.038	1.06	1.44	7.0	Easy flowing
Al_2O_3–TiO_2 spray-dried powder	0.023	0.02	0.25	40.0	Free flowing

Acknowledgements

This work has been supported by the Spanish Ministry of Economy and Competitiveness (MAT2009-14144-C03-01, MAT2012-38364-C03-01 and MAT2012-31090).

References

[1] E. Sánchez, M. Vicent, A. Moreno, M.D. Salvador, E. Klyatskina, V. Bonache, I. Santacruz, R. Moreno, Preparation and spray-drying of nanoparticle Al_2O_3–TiO_2 suspensions to obtain nanostructures coatings by APS, Surface and Coatings Technology 205 (2010) 987–992.
[2] N. Dejang, A. Watcharapasorn, S. Wirojupatump, P. Niranatlumpong, S. Jiansirisomboon, Fabrication and properties of plasma-sprayed Al_2O_3/TiO_2 composite coatings: a role of nano-sized TiO_2 addition, Surface and Coatings Technology 204 (2009) 1651–1657.
[3] M. Vicent, E. Bannier, R. Benavente, M.D. Salvador, T. Molina, R. Moreno, E. Sánchez, Influence of the feedstock characteristics on the microstructure and properties of Al_2O_3–TiO_2 plasma-sprayed coatings, Surface and Coatings Technology 220 (2013) 74–79.
[4] X.Q. Cao, R. Vassen, S. Schwartz, W. Jungen, F. Tietz, D. Stöever, Spray-drying of ceramics for plasma-spray coating, Journal of the European Ceramic Society 20 (2000) 2433–2439.
[5] N. Berger-Keller, G. Bertrand, C. Filiare, C. Meunier, C. Coddet, Microstructure of plasma-sprayed titania coatings deposited from spray-dried powder, Surface and Coatings Technology 168 (2003) 281–290.
[6] B. Faure, J.S. Lindeløv, M. Wahlberg, N. Adkins, P. Jackson, L. Bergström, Spray drying of TiO_2 nanoparticles into redispersible granules, Powder Technology 203 (2010) 384–388.
[7] S. Fazio, J. Guzmán, M.T. Colomer, A. Salomoni, R. Moreno, Colloidal stability of nanosized titania aqueous suspensions, Journal of the European Ceramic Society 28 (2008) 2171–2176.
[8] M. Vicent, E. Sánchez, I. Santacruz, R. Moreno, Dispersion of TiO_2 nanopowders to obtain homogeneous nanostructured granules by spray-drying, Journal of the European Ceramic Society 31 (2011) 1413–1419.
[9] M. Vicent, E. Sánchez, A. Moreno, R. Moreno, Preparation of high solids content nano-titania suspensions to obtain spray-dried nanostructured powders for atmospheric plasma spraying, Journal of the European Ceramic Society 32 (2012) 185–194.
[10] T. Molina, M. Vicent, E. Sánchez, R. Moreno, Dispersion and reaction sintering of alumina–titania mixtures, Materials Research Bulletin 47 (2012) 2469–2474.
[11] C. Schilde, C. Mages-Sauter, A. Kwade, H.P. Schuchmann, Efficiency of different dispersing devices for dispersing nanosized silica and alumina, Powder Technology 207 (2011) 353–361.
[12] A.R. Studart, E. Amstad, L.J. Gauckler, Colloidal stabilization of nanoparticles in concentrated suspensions, Langmuir 23 (2007) 1081–1090.
[13] S. Jailani, G.V. Franks, T.W. Healy, ζ potential of nanoparticle suspensions: effect of electrolyte, concentration, particle size, and volume fraction, Journal of the American Ceramic Society 91 (2008) 1141–1147.
[14] T. Ohno, K. Sarukawa, K. Tokieda, M. Matsumura, Morphology of a TiO_2 photocatalyst (Degussa P-25) consisting of anatase and rutile crystalline phases, Journal of Catalysis 203 (2001) 82–86.
[15] J.L. Amorós, A. Blasco, J.E. Enrique, F. Negre, Características de polvos cerámicos para prensado (Characteristics of ceramic powders for pressing), Boletín de la Sociedad Española de Ceramica y Vidrio 26 (1987) 31–37.
[16] J. Schwedes, Review on testers for measuring flow properties of bulk solids, Granular Matter 5 (2003) 1–43.
[17] A.W. Jenike, J.R. Johanson, Review of the principles of flow of bulk solids, CIM Transactions 73 (1970) 141–146.
[18] P. Fauchais, G. Montavon, G. Bertrand, From powders to thermally sprayed coatings, Journal of Thermal Spray Technology 19 (2010) 56–80.
[19] P. Fauchais, G. Montavon, R.S. Lima, B.R. Marple, Engineering a new class of thermal spray nano-based microstructures from agglomerated nanostructured particles, suspensions and solutions: an invited review, Journal of Physics D: Applied Physics 44 (2011) 093001 http://dx.doi.org/10.1088/0022-3727/44/9/093001.
[20] Y. De Hazan, J. Heinecke, A. Weber, T. Graule, High solids loading ceramic colloidal dispersions in UV curable media via comb-polyelectrolyte surfactant, Journal of Colloids and Interface Science 337 (2009) 66–74.
[21] J.L. Amorós, J.G. Mallol, B. Campos, M.J. Orts, M.C. Bordes, Study of the rheological behaviour of different ceramic powder materials, part 1, Interceramics 57 (2008) 236–239.
[22] J.L. Amorós, J.G. Mallol, B. Campos, M.J. Orts, M.C. Bordes, Study of the rheological behaviour of different ceramic powder materials, part 2, Interceramics 57 (2008) 314–316.
[23] J.A.H. Jong, A.C. Hoffmann, H.J. Finkers, Properly determine powder flowability to maximize plant output, Chemical Engineering Progress 95 (1999) 25–34.